Open Access

Catalysis Research

LIDSEN Publishing Inc.

Research Article

The Effects of Ge Substrate Surface States and Au Catalyst Layer Thickness on the Growth of Different Ge_xO_y Nanomaterials and Nanocrystals Configurations Using Vapor-Liquid-Solid Method with two Steps Temperature Mode

Khac An DAO [1, 2, ‡, *], Hong Trang PHAM [3, †], Van Vuong HOANG [4, †]

1. Institute of Theoretical and Applied Research (ITAR), Duy Tan University, Hanoi 100000, Vietnam; E-Mails: daokhacan@duytan.edu.vn; andaokhac@gmail.com
2. Faculty of Electrical and electronics Engineering, Duy Tan University, Da Nang, 550000, Vietnam; E-Mails: daokhacan@duytan.edu.vn; andaokhac@gmail.com
3. Co-worker of EMD Lab., Institute of Materials Science (IMS), VAST, 18 Hoang Quoc Viet Road, Cau Giay, Hanoi, Vietnam; E-Mail: trangpham8405@gmail.com
4. Department of Materials Science, Heat and Surface, School of Materials Science and Engineering, Hanoi University of Science and Technology (HUST), Vietnam; E-Mail: Vuonghvbk@gmail.com

‡ Current Affiliation: Institute of theoretical and applied Research (ITAR), Duy Tan University, Ha Noi 100000 Vietnam, CT1 Trang An complex, No1 Phung Chi Kien street, Cau Giay Hanoi

† These authors contributed equally to this work.

* **Correspondence:** Khac An DAO; E-Mails: daokhacan@duytan.edu.vn; andaokhac@gmail.com

Academic Editor: Narendra Kumar

Special Issue: Nanoparticles and Nanotechnologies in Catalysis

Catalysis Research
2023, volume 3, issue 1
doi:10.21926/cr.2301006

Received: September 01, 2022
Accepted: January 17, 2023
Published: January 31, 2023

Abstract

Recently the Ge_xO_y nanomaterials have been studying intensively due to their interesting electronic materials, which have many particular properties and applications in nanotechnology and nano-devices fabrication. Much work has been done on many different

synthesis methods and their properties of Ge and Ge_xO_y nanomaterials. However, the effects of the different Ge substrate surface states and Au catalyst layer thicknesses on the formation of different forms/morphologies of nanomaterials (nanowires, nanorods, nanoparticles, and nanocrystals particularly) have not yet to be discussed more in detail. This paper outlines the synthesis methods to grow the different Ge_xO_y nanomaterials on the different Ge surface states at different Au catalyst layer thicknesses such as mechanically polished surface, deep Chemical etched surface, chemical polishing surface, and initial rough surface. The morphological, and structural properties of Ge_xO_y nanomaterials have been investigated using SEM, EDX, and TEM techniques. The formation of different morphological, and structural properties of different Ge_xO_y nanomaterials grown have been explained by the effects of the Au/Ge/O droplets/clusters formation situations and surface defects on the Ge substrate surface caused. The growth mechanisms have been explained by the model of the VLS growth method with the Oxide Assist Growth mechanism. The results showed that the effects of the different Ge substrate surface states and Au catalyst layers' thickness strongly influence the formation of Ge_xO_y materials in terms of the sizes, structures, and percentages of elements. The results of the controllable different Ge_xO_y nanomaterials have many significant meanings for both theoretical and practical applications in nanomaterials and nano-device fabrication.

Keywords

The Ge substrate surface states' effects on Ge_xO_y growth; different Ge_xO_y nanomaterials growth and control; big multifacial Nanocrystal growth; the catalyst layer thicknesses effects; VLS method with two steps temperature mode

1. Introduction

The nanostructured materials, including the nano thin-films (NTFs), nanowires (NWs), nanorods (NRs), nanoparticles (NPs), and recently nanocrystals (NCs), have been playing a significant role in the theoretical and practical researches for various applications in nanotechnology and nanodevices [1-4]. So far there are two main technological approaches to fabricating semiconductor nanomaterials: the top-down technology and the bottom-up technology [4], where the bottom-up technology recently is an interesting approach that has been widely used for the synthesis of the different Ge, Si, and GaAs semiconductor nanomaterials configurations by various methods [4, 5] such as by the Vapor-Liquid-Solid (VLS) method with one or two steps temperature mode [4-7], by the chemical vapor deposition (CVD), by the plasma-assisted CVD [8, 9], by the laser ablation [10], by Molecular Beam Epitaxy (MBE) [11], and other methods via simple vapor transport [12]. Among them, the VLS method is widely used because the VLS growth method can better control nanowire sizes by controlling the sizes of growth seeds. This method is low-cost and versatile and can produce different nanomaterials types with several morphologies, orientations, and compositions. In addition, recently F. Panciera et al. [13] still reported and introduced a technique that extends the VLS method of nanowire growth, allowing the formation of nanowires that contain embedded nanocrystals, i.e., the catalyst particle is used not only to grow nanowires but in an extended role, to nucleate different nanocrystals independently. Notably, the VLS method was also widely used to

synthesize the Ge nanomaterials in different forms with the variations of two-step temperature mode can make at the below or above the eutectic Temperature of the relative binary system, combining technological conditions including the Au catalyst layer thickness that can also control the nanomaterials morphologies and modify the growth mechanisms, even one can use the VLS method to explain many new interactions, including the remarkable new effects between the metal catalyst and semiconductor [14-21].

Concerning the Ge nanowire growth, since 1993 the first work by James R et al. [5] reported about the solution-phase synthesis of Ge nanowires, up to recently, there have been being many works outlined on the different theoretical and experimental results concerning the various aspects of synthesis, properties of Ge nanomaterials as well as the influences of growth conditions on Ge nanomaterials morphologies, such as the growth of individual vertical Germanium nanowires [14], the formation of the hexagonal close-packed structure of Au Nano catalysts after Ge nanowire VLS growth [15], the effects of surface oxide formation on germanium nanowire [16], the structural of amorphous, crystalline and liquid GeO_2 [17], surface characterization of oxide growth on porous germanium films oxidized in the air [18], the synthesis and characterization of germanates [19], the effects of morphology and composition of Au catalysts on Ge (111) by thermal dewetting [20], the role of Surface Passivation in Controlling Ge Nanowire Faceting [21] and the growth of Ge NWs below the eutectic temperature together some problems concerning also have been reported in several works [22-25].

The focused attention on Ge NWs recently is mainly owing to their higher intrinsic carrier mobility, high intrinsic carrier concentrations, larger bulk excitonic Bohr radii, bandgap control of nanostructures, compatibility with higher dielectric constant materials that are promising applications for faster switching and high-frequency devices, field-effect transistor, IR detector, more prominent quantum confinement effects for photoluminescent studies, enabling integration with current semiconductor technology. Ge nanowires (Ge NWs) satisfy both criteria of new material with novel structures. Although many aspects of synthesis and experimental results have been investigated and also reported on the properties and morphologies of Ge NWs, *unfortunately, only a few works have reported, discussed, and remarked on the dominant roles of different Ge substrate surfaces on nanowires*, so far there was a work of Chuanbo Li, et al. [11] mentioned shortly that the growth of Ge nanowires was quite sensitive to the surface condition of the substrate, a clear understanding of this phenomenon could help us engineer the growth of nanowires. Although so, there are no more research works found that dealt with the impacts of the different Ge substrate surface states together with Au catalyst layer thickness on the growth of different sizes Ge_xO_y nanomaterials, including NWs, NRs, NPs, and NCs configurations as well as the abilities for the control of their morphologies and sizes.

In this paper, we comprehensively outline the synthesis process for the growth of different Ge_xO_y nanomaterials (NPs, NWs, NRs, and multi-facial configurations here so-called nanocrystals), the abilities for controlling their sizes and morphologies depending on the Ge substrate surface states and Au catalyst layers' thickness could be achieved by using VLS method with two-steps temperature profile above eutectic temperature of Au-Ge binary system. The growth formation mechanism, structural properties, and morphologies for the different Ge nanomaterials configurations have also been studied and discussed.

2. Materials and Methods

2.1 The Materials and Preparation of the Different Ge Substrate Surface States Samples Groups

Starting materials were the rough surface Ge slices with n-type, (111) orientation, and resistivity of about 1 Ω.cm obtained from a commercial company. The chemical treatment process involved several steps. In the first step, Ge slices were cut into several small-size specimens of square with 5 mm and 5 mm sides and then cleaned chemically by ultrasonic vibration in three solutions alternatively: acetone (CH_3COCH_3 99.5%), solution of alcohol (CH_3CH_2OH 95%), and ionized water for 5 minutes (mins). In the second step, using a chemical treatment, the specimens were cleaned the dust/oil being on the substrate by immersing Ge specimens in the solution of DI water: HCl with a volume ratio of 3:1 then removed HCl and cleaned by using an Ultrasonic vibration process in acetone and alcohol. The last procedure involved vibrating in the ionized water and drying. In the final step, all cleaned Ge specimens were divided into four groups. Each group was treated differently to get different surface states, as shown in Figure 1.

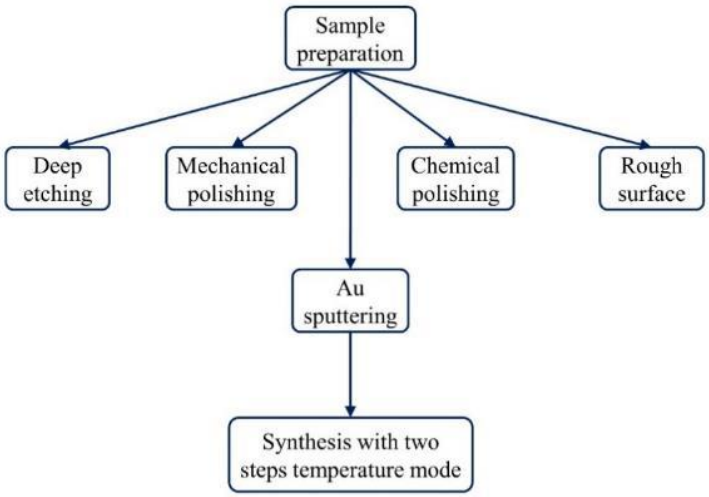

Figure 1 The process of sample preparation for different groups.

Group 1 with Mechanical Polishing surface samples: the initially rough surface samples were mechanically polished with 1 µm felt cloth until they became fully flat glossy surfaces with almost no scratch can be seen under microscopy. The Ge substrate surface of this group is the finest.

Group 2 with chemical polishing: The samples were treated by a soft etching-polishing method using HNO_3 (68%): HF (37%) with a ratio of 5:3 for 1.5 mins. The Ge substrate surface of this group is rather slightly smooth-fine but contains small pits-bumps. *Group 3 with deep Chemical etching surface samples*: the samples were treated and then chemically etched using the mixed solution of DI water: H_2O_2 (30%): HCl (37%) with a ratio of 6:1:1 in 1.5 mins. The Ge substrate surface of this group contains a larger pits-bumps surface than the other group's Ge substrate surface. *Group 4 with Ge rough surface*: These samples are the initial Ge samples obtained from the commercial company. Their surface has a certain roughness and long traces, grave defect under Ge surface caused by the slice sawing.

Briefly, in Group 1: Mechanical Polishing samples have the best fine surface; in Group 2: Chemical polishing surface samples have rather delicate surfaces; in Group 3: Deep chemical etching surface

samples have the most pits-bumpy defective etching surface; and in Group 4: Initial rough surface samples have initial–original rough surface after sawing slices and chemically treated by the manufacturer company where there are some acceptable deep defects caused by sawing process and chemical treatment. After the treatment of the different Ge substrate surface states, all samples have taken to be sputtered with the 50 nm and 130 nm different thin Au layers thicknesses onto all Ge samples' front side surface. The thickness of Au thin layers was measured using the SEM cross-section method and Teli step equipment. Figure 2 shows the surface states of four sample groups before and after the deposition of the Au thin film layer in comparison.

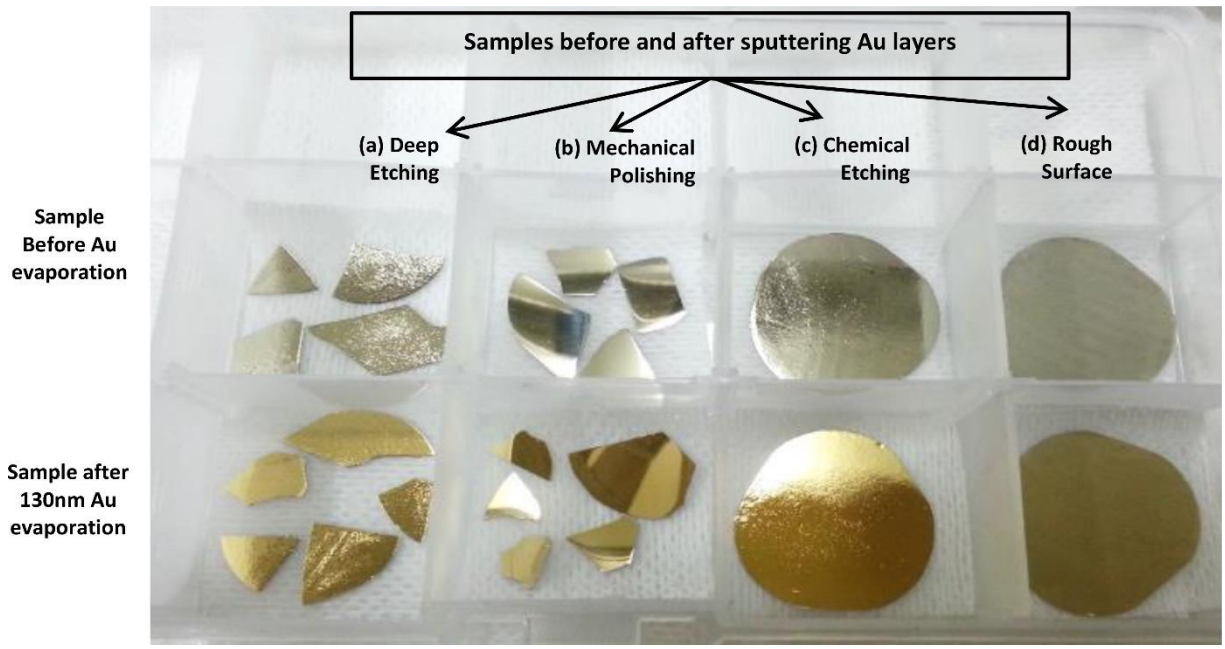

Figure 2 The Photographs of samples showing the surface states of four samples groups before and after Au sputtering onto the different Ge substrate surface states: Deep Etching with large pits-bumps, defective, not smooths surface (a), Mechanical Polishing with the finest surface (b), Chemical polishing with relatively slight smooth-fine but it contains small pits-bumps (c); and the initial rough surface with a certain roughness, long traces-deep defect caused by the slice sawing process and initial chemical treatment (d).

2.2 The Ge_xO_y Nanomaterials Growths on the Different Ge Substrate Surface States Samples

After preparation of different Ge substrate surface states, the Ge_xO_y nanomaterials growths have carried out in the 10^{-1} to 10^{-2} Torr low vacuum Lindberg/Blue M Three-zone tube Furnace as in Figure 3 (a, b) with the temperature diagram as in Figure 3(c). The experimental temperature curve of two steps temperature profile was measured by a thermal couple connecting with PC via Keithney2000 multimeters, as shown in Figure 3(d).

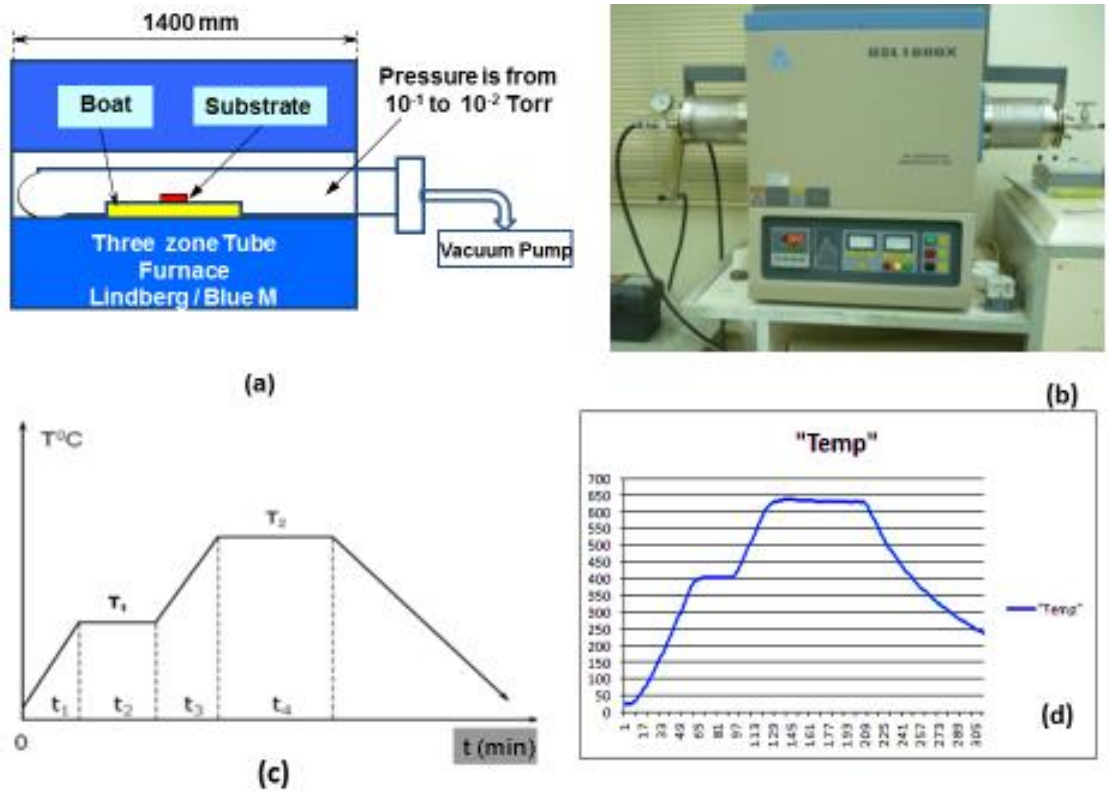

Figure 3 Block scheme of experiment equipment furnace with the pressure (P) inside of tube is 10^{-2} Torr (a), the photo image of Lindberg/Blue M Three-zone tube Furnace b), and thermal VLS method with two steps temperature mode (c), and an example of the measured temperature profile (d).

The growth processes of Ge_xO_y configurations for the different sample groups with different surface states were experimentally repeated using the thermal annealing VLS method with two-step temperature mode over the Eutectic temperature of Au and Ge binary system under various technological conditions. SEM, EDX, and TEM techniques have investigated samples' morphological and structural properties.

Here we would like to emphasize that the thermal VLS method used here with a two-step temperature mode: the annealing temperature T1 was set constantly at 400°C for the disturb of the Au catalyst layer, which is higher than the Eutectic temperature (361°C) of the Ge-Au binary system. The second temperature mode was set differently, with T2 temperature varying from T2 = 620°C to 720°C with the growing time duration variation of t4 = 55-125 minutes (mins). The labeled sample groups, Au layer thickness, and the technical conditions are listed in Table 1. The technological conditions for all growth processes are different, aiming to investigate the influences of the different substrate surface states at two 50 nm and 130 nm thicknesses of Au metal catalyst layers.

Table 1 Technological conditions for growing the different Ge_xO_y nanomaterials on Ge substrates with different surface states.

Samples Groups	Au layer thickness (nm)	Sample label	t_1 (mins)	T_1 (°C)	t_2 (mins)	t_3 (mins)	T_2 (°C)	t_4 (mins)
Group1: Mechanical polishing surface Samples	25	M1	55	400	75	34	620	60
	25	M2	55	400	75	34	620	125
	30	M3	55	400	75	50	720	60
	50	M4	55	400	75	34	620	60
	50	M5	55	400	75	34	720	90
	130	M6	55	400	75	34	620	90
Group 2: Chemical polishing surface samples	50	M7	55	400	75	34	620	90
	130	M8	55	400	75	34	620	90
Group 3: Deep Chemical etching surface samples	50	M9	55	400	75	34	620	90
	130	M10	55	400	75	34	620	90
Group 4: Initial Rough Surface samples	50	M11	55	400	75	34	620	90
	130	M12	55	400	75	34	620	90

3. The Experiment Results

The obtained experimental results for growths and properties investigations of the Ge_xO_y nanomaterials on the different Ge substrate surface states with different Au catalyst layers' thicknesses at the given technological conditions can be seen from Figure 3 to Figure 18. It is worth noting that here we denote the grown nanomaterials configurations commonly by the symposium of Ge_xO_y (where x≡ 1, 2, 3 and y≡ 1, 2, 3; depending on growing in the nanoscale sizes and classic materials systems, the values of x, y could be received values smaller or larger than 1).

3.1 The Grown Results of Ge_xO_y Nanomaterials on the Mechanical Polishing Surface Samples with Different Au Catalyst Layer Thicknesses at Different Technological Conditions

The grown technological conditions for mechanical polishing surface samples (Group 1) can be seen in Table 1. In the case of the Au catalyst layer thickness sputtered on the Ge substrate is smaller than 30 nm, the tiny Au droplets will be formed on the Ge polishing surface with supersaturation levels, and the small nano seeds will also be formed during thermal annealing processes at T1 and T2 temperatures, consequently, *there are small tangle forms NWs configurations* grown with small – extended sizes on M1, M2, and M3 samples as showing in Figure 4. In addition, we also see that in the case of the longer growing time (t_4 = 125 mins) for the M2 sample, there are few spherical configurations of so-called nanocrystals also formed, here their sizes are about 400-600 nm, their growing mechanism is hard to explain. The sizes of NWs in these cases are about 100 nm for M1

and M2 samples with 25 nm Au layer thickness and increased to about 200 nm for the M3 sample with 30 nm Au layer thickness. These obtained results agree with the results reported in many published works [4-8].

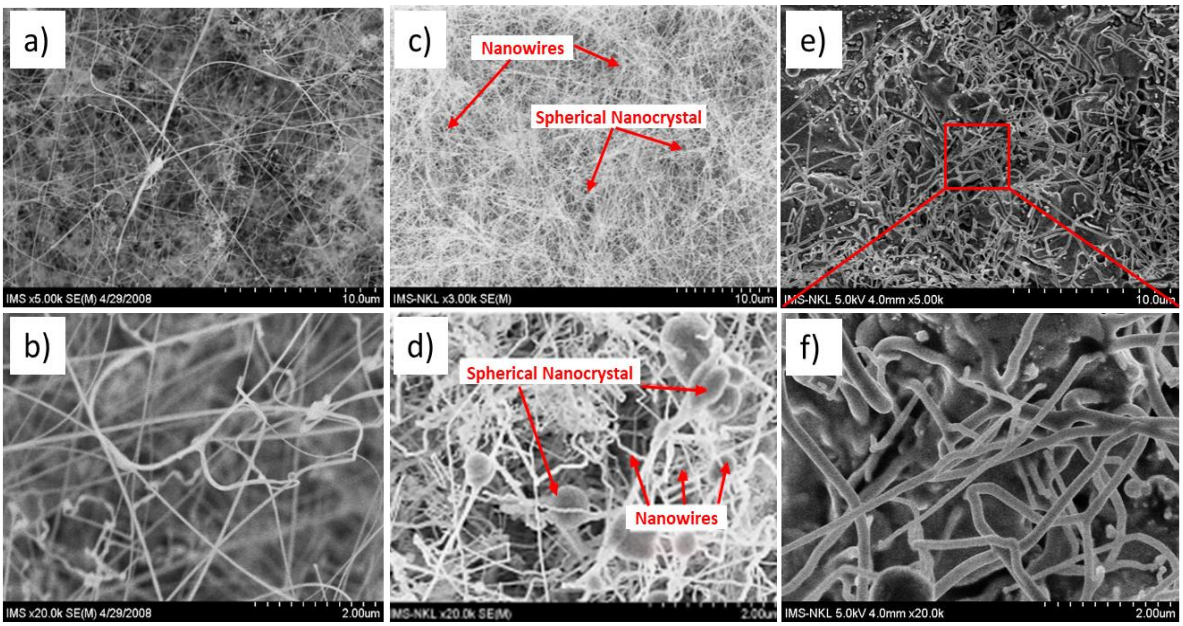

Figure 4 FESEM micrographs of NWs grown on the samples of thin Au catalyst layer thicknesses at different growing temperatures (T2) and growing times (t4) (see in Table 1): NWs grown on M1 sample with 25 nm Au laer thickness for different magnitifications (a, b); NWs together with several NCs grown on M2 sample with 25 nm Au thickness for long growing time with different magiifications (c, d); and bigger NWs grown on M3 sample for the case of 30 nm Au thickness with different magiifications (e, f).

When the Au catalyst layer thickness increased to 50 nm for samples of M4 and grew at a temperature of T2 = 620°C with growing time t4 = 60 mins for M4, then the mixed different sizes Ge_xO_y configurations including NPs, NWs, NRs, and NCs were dominantly grown on M4 sample. The NWs and NRs have diameters of about 100 nm to 200 nm while the sizes of multifacial and spherical NCs are about 400 nm to 600 nm, see on Figures 5 a, b) in below.

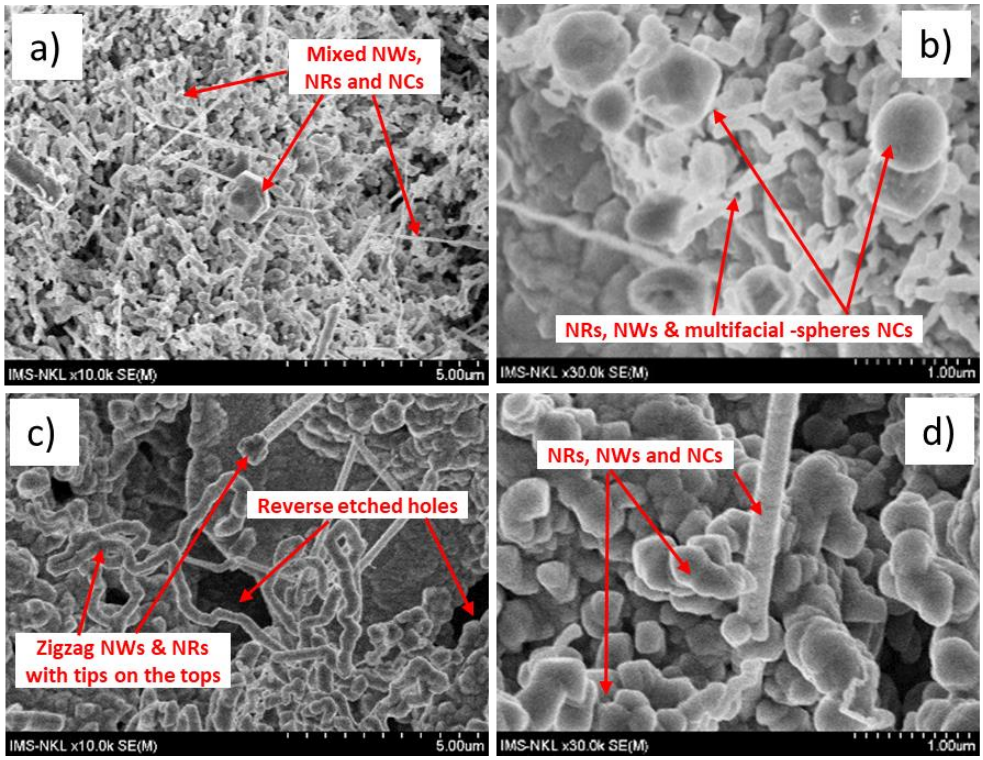

Figure 5 FESEM micrographs of the mixed grown configurations of NRs, NWs together with multifacial configurations so called NCs at different magnifications grown on sample M4 (a, b) and FESEM of the zigzag NWs and reverse etched holes (c) and the NRs, multifacial NPs-NCs grown on M5 sample (d). The technological conditions for growing nano configurations are outlined in Table 1.

For the case of the M5 sample with Au catalyst layer thickness of 50 nm, but when the growth temperature increased to T2 = 720°C with longer growing time, t4 = 90 mins, then the mixed different nano configurations (consisting of NRs, NWs, NPs) grown on M5 sample with the sizes of about 300 nm-400 nm (Figure 5c) and nanorods, multifacical configurations have sizes about 400 nm-500 nm (Figure 5d), and especially under the higher growing Temperature together with thicker Au Catalyst *layer there were several deep holes formed on the Ge substrate, the reverse etching process explains this phenomenon into the* Ge substrate (Figure 5c) occurred. From the results of Figure 4 and Figure 5, we can state that depending on Au catalyst layer thickness and growing temperature T2, we can grow the single or mixed nanomaterials configurations of NWs, NRs, NPs, and NCs with different sizes.

Figure 6 (a) shows the results of the energy-dispersive X-ray spectroscopy (EDX) of the NWs on the M3 sample (group 1) with 30 nm Au catalyst layer thickness. The chemical composition of the nanowire consists of two elements Germanium (Ge) and oxygen (O), with the percentage of atoms: Ge (34.84%) / O (65.16%) ratio is Ge: O = 1/1.87, so the NWs composition, in this case, is $Ge_{1O1.87}$ (x = 1, y = 1.87 < 2). This result often occurs in the nano process. Figure 5(b) shows the EDX result of the structural formula of nanowires on M4, and this result showed that when the growing temperature (T2) changed and the Au catalyst layer increased to 50 nm, then the ratio *of* Ge (31.98%) / O (68.02%) is Ge: O = 1/2.12 (x = 1, y = 2.12.2). In this case, the Ge_xO_y has the ratio of $Ge_1O_{2,12}$ this ratio has a decimal number. *So we see that the technological conditions and Au catalyst layer* thickness will determine the composition and form of Ge_xO_y nanomaterials.

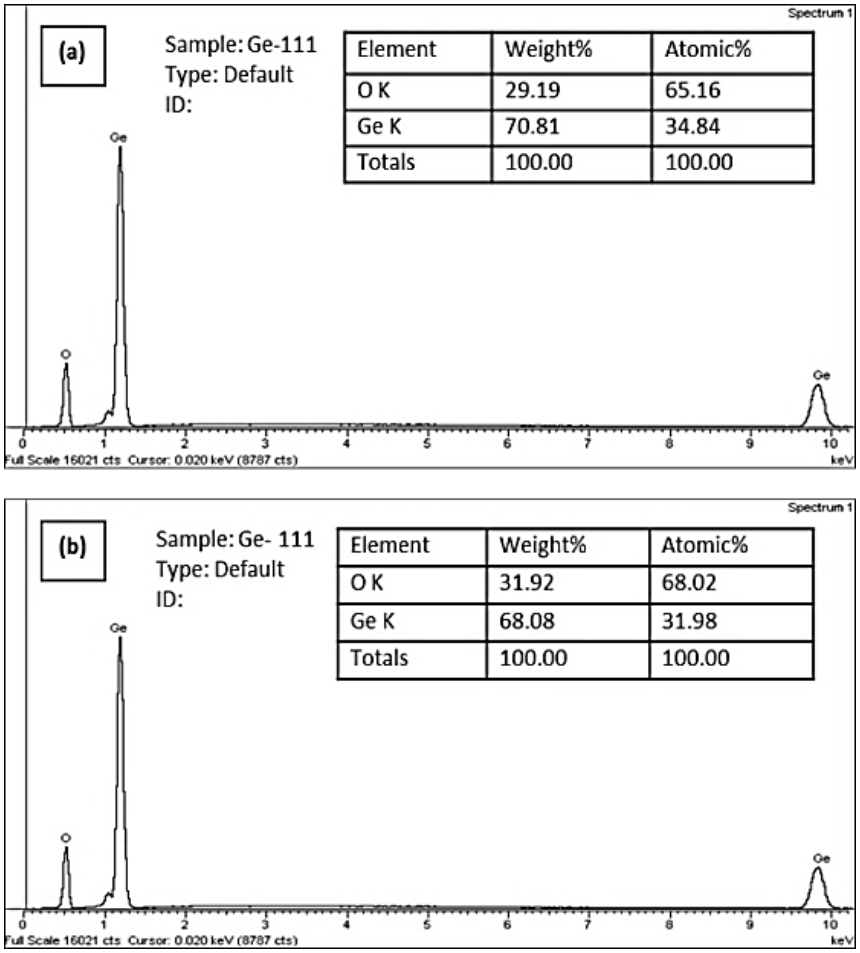

Figure 6 EDX image of Ge nanowires on M3 sample with the composition of $Ge_1O_{1.87}$ (a) and on M4 sample with the composition of $Ge_1O_{2.12}$ (b).

Figure 7 shows TEM micrographs of a zigzag NW on an M5 sample with different magnifications. Figure 7a) shows a TEM image of a part of NW with a size of about 500 nm. Figure 7b) shows an enlarged end part of the NW; there are several discrete dark circles observed here, and in the enlarged TEM image of Figure 7c), *these circles are assumed to be Ge_xO_y crystalline structures*. Here we can see that the NW has two parts: the core and the shell parts. The FFT (Fast Fourier Transform) result (Figure 7d) showed that the shell has a structure of the amorphous phase containing the discrete crystalline structures circles.

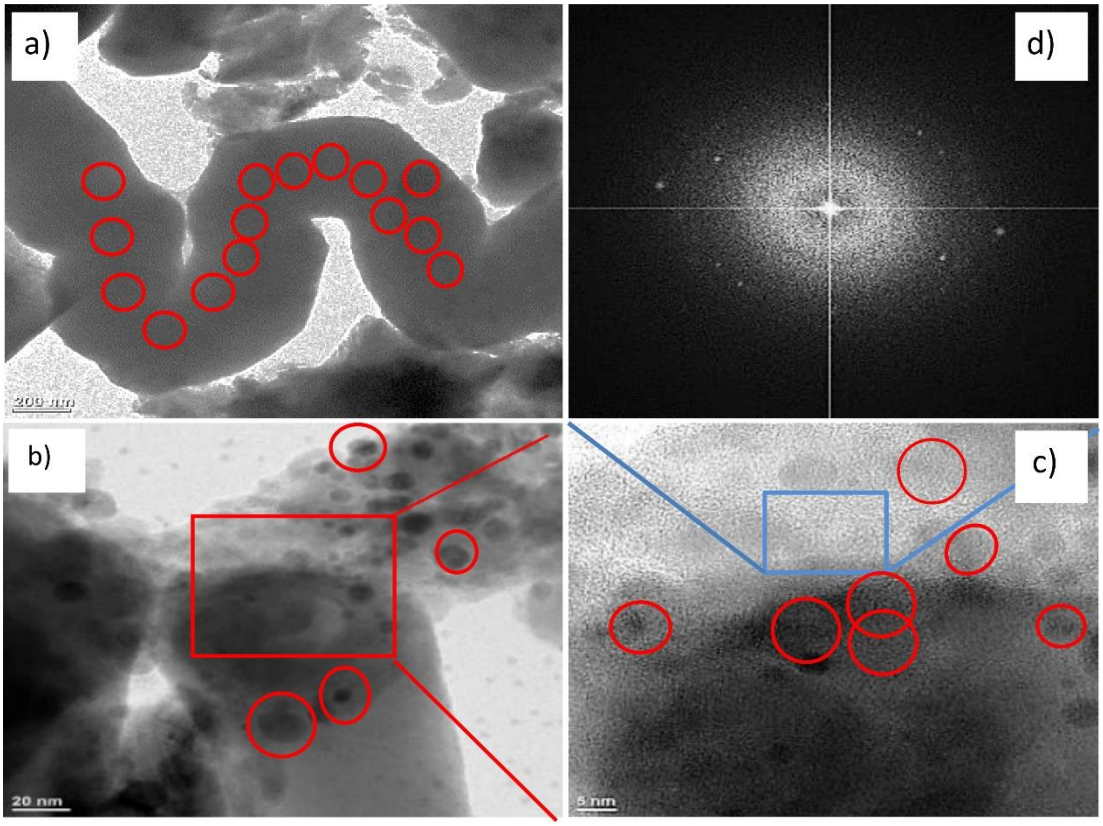

Figure 7 TEM micrographs of the mechanical polishing surface M5 sample: Image of a zigzag NW part with size of about 500 nm (a), the magnified images in the different regions of NW (b, c). The FFT results showed that the structural feature in this region is amorphous phase.

Regarding the M6 mechanical polishing surface sample with a much thicker Au catalyst layer thickness of 130 nm, we observed multifacial configurations, *so-called Nanocrystals (NCs)* grown with a big size of about 1 µm to 2 µm, as shown in Figure 8. There were no NWs grown that can be found.

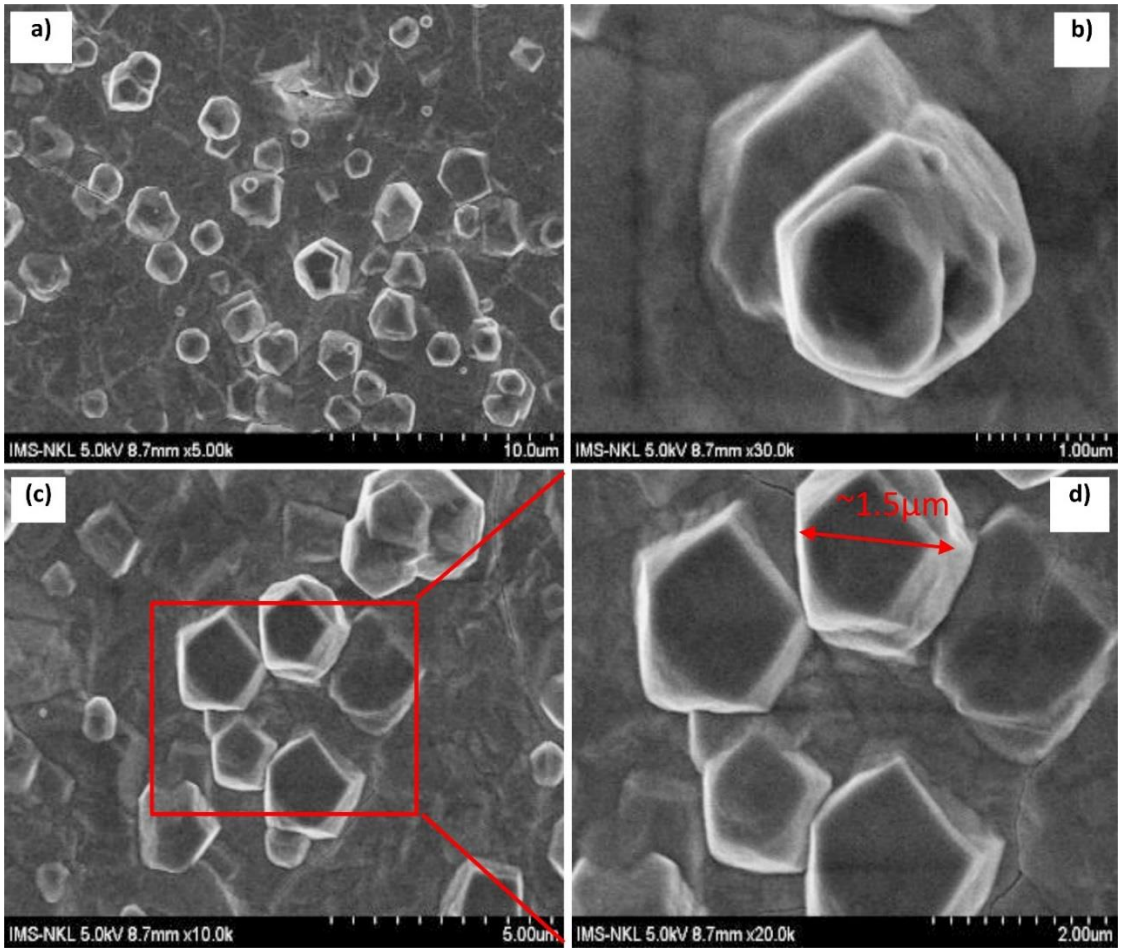

Figure 8 FESEM micrographs of the multifacial configurations so called NCs grown on Mechanical polishing surface sample M6 with thick Au catalyst layer of 130 nm, growing temperature T2 = 620°C for growing time t4 = 30 mins time (see in Table 1).

Figure 9 shows the TEM micrographs of a multifacial nano configuration (NCs) grown on the mechanical polishing surface M6 sample with an Au catalyst layer thickness of 130 nm. As the nano multi-facial configuration is too thick it is hard to prepare enough thin samples for TEM investigation; we could only investigate-measure the cross-sectional TEM micrographs at its edge where the thickness is thin enough for the TEM investigation.

The investigated results in Figure 9 (a) showed the typical multifacial NCs configuration. We see that the NCs structure has a cover-shell layer with a size of about 5-6 nm; the structure of the shell layer is amorphous, as shown in Figures 9 b, e). The core of NC is a crystalline structure (Figure 9d) with insert HR–TEM image from the indicated box (Figure 8b). The inset shows the corresponding pattern recorded along with the (200), (111), and (022) orientations. The atoms layer space is 0.334 and 0.294 nm, as shown in Figure 9c).

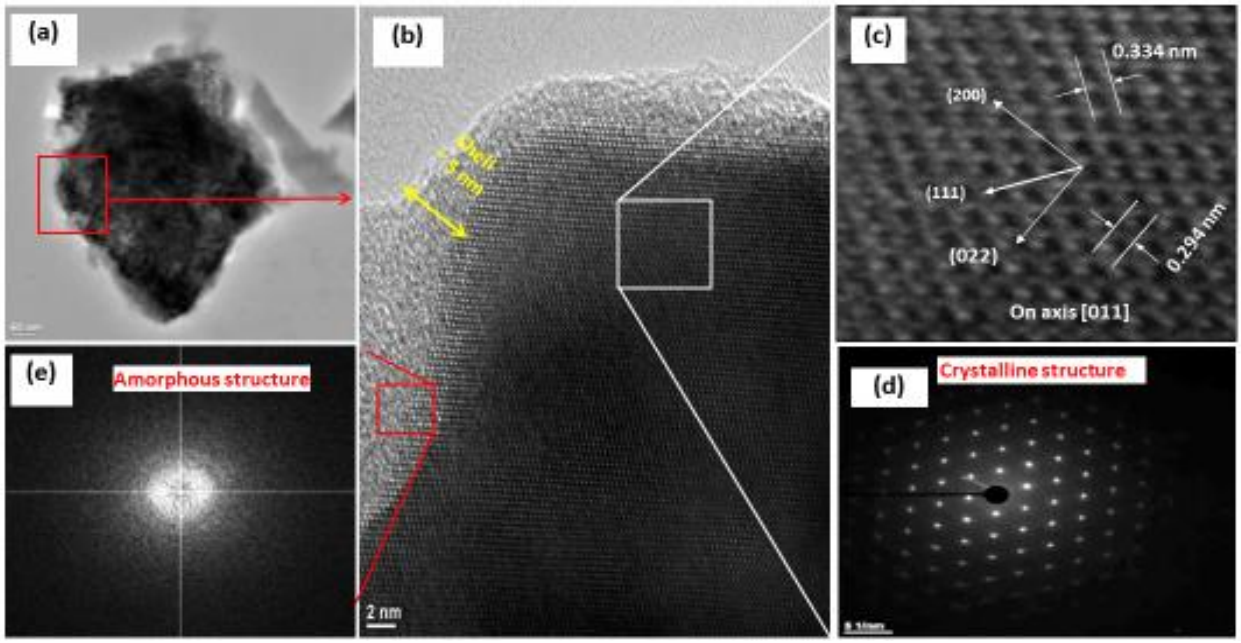

Figure 9 HRTEM micrograph images of an NC configuration being on M6 sample with the mechanical polishing surface sample. The NC has the shell and core parts: the core structure is crystalline (b, c, d), and the shell layer structure is amorphous with a size is about 5 nm-6 nm (b, e).

3.2 The Grown Results of Ge_xO_y Nanomaterials Configurations on the Chemical Polishing Surface Samples with Different Au Catalyst Layer Thickness at Different Technological Conditions

Regarding the nanomaterials grown on the chemical polishing samples containing minor defects produced by chemical etching with a rather fine-less smooth surface as shown in Figure 2c. Figure 10 shows typical results of the nanomaterials grown on the M7 sample with the Au catalyst layer thickness of 50 nm at growing temperature T2 = 620°C and t_4 = 120 mins. Here we see that the mixed configurations grown with the bigger size Ge_xO_y NWs configurations, their sizes are in the range of from 500 nm to 600 nm in diameter with big spheres configurations of 1000-1500 nm sizes located on the tops of NWs (Figure 10 a, b, c).

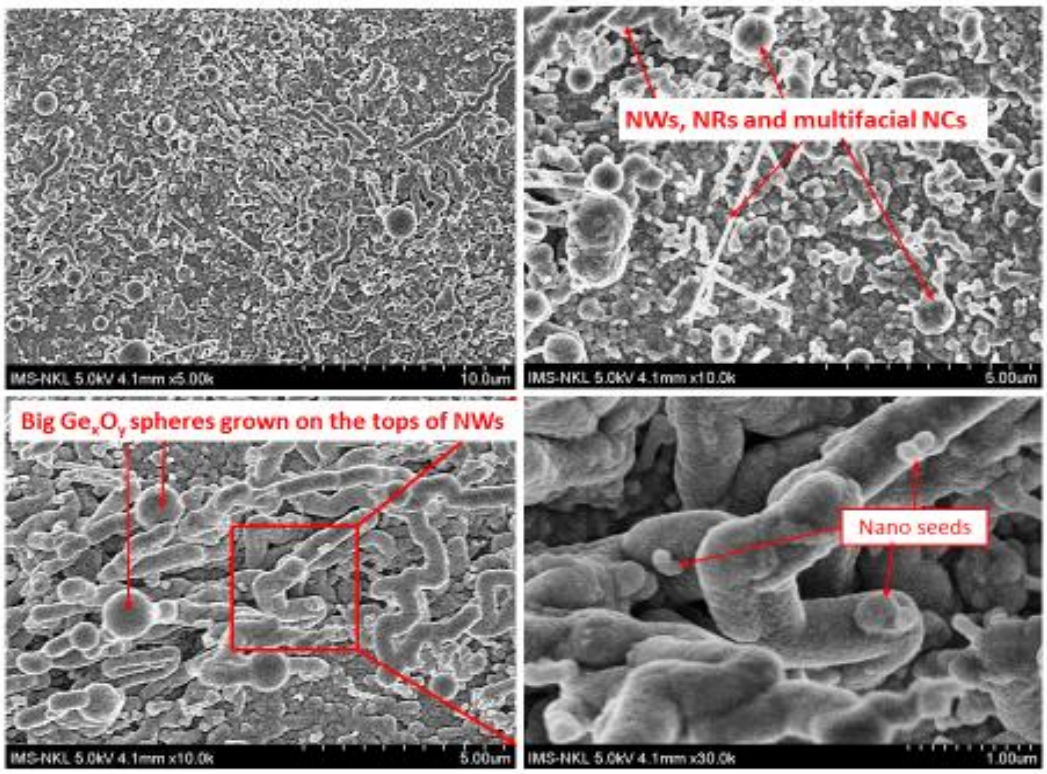

Figure 10 SEM micrographs of Ge nanomaterials (NPs, NWs, NRs) configurations grown on the chemical polishing surface M7 sample with the sputtered 50 nm Au catalysis layer.

The growth of the bigger NWs and spheres configurations on the tops of NWs in the chemical polishing surface state (Figure 10) occurred more in comparison with that of the case in the mechanical polishing surface M5 sample (Figure 5). We have tried to study the structure-property of the grown big-size nanowires configuration of M7. However, which has a thick sample, it is hard to determine clearly. Here we also observed that the big spheres formed and located on the tops of NWs (Figures 10 a, b, c); these spheres have the same color as that of the NWs they located; from this fact, *we could assume that the compositions of these big spheres are assumed to be the same as the compositions of Ge_xO_y NWs related. This evidence shows that the growth mechanism in this case is not grown by the initial VLS mechanism but is explained by the foreign Au catalyst element mediated Oxide Assisted Growth (OAG) mechanism proposed by the author's works* [26-29].

Figure 11 shows the FESEM and TEM micrographs of an NWs configuration grown on the chemical polishing surface M7 sample with the Au catalyst layer thickness of 50 nm (Group 2): the FESEM image of the NWs configurations is shown in Figure 11a). Figure 11b) shows the TEM micrograph on the tip of an NW configuration and Figure 11 c) shows the tip's magnified TEM image. *Here we see that the NW tip contains the separated small black spheres that are assumed to be small Ge_xO_y clusters or nanocrystal seeds formed during the growing process* [29, 30]. The FFT result shows that the marked region in the tip of NW in Figure 11c) that has an amorphous structural feature (Figure 11d). The TEM image of the NW body part is shown in Figure 11e), this NW part consists of the core part with a diameter size of about 120-130 nm and an ununiformed sheath (shell) with a size of 50-70 nm. The FFT result of the marked box shows that the region in the NW body has an amorphous structural feature (Figure 11f). We can see that there are many small dark circles configurations with sizes of 1-3 nm; these are located inside the NW body and a sheath. We suppose

that these are nanocrystal seeds formed and moved up to build NW growth based on the growth mechanism model proposed by Noor Mohammad et al [30].

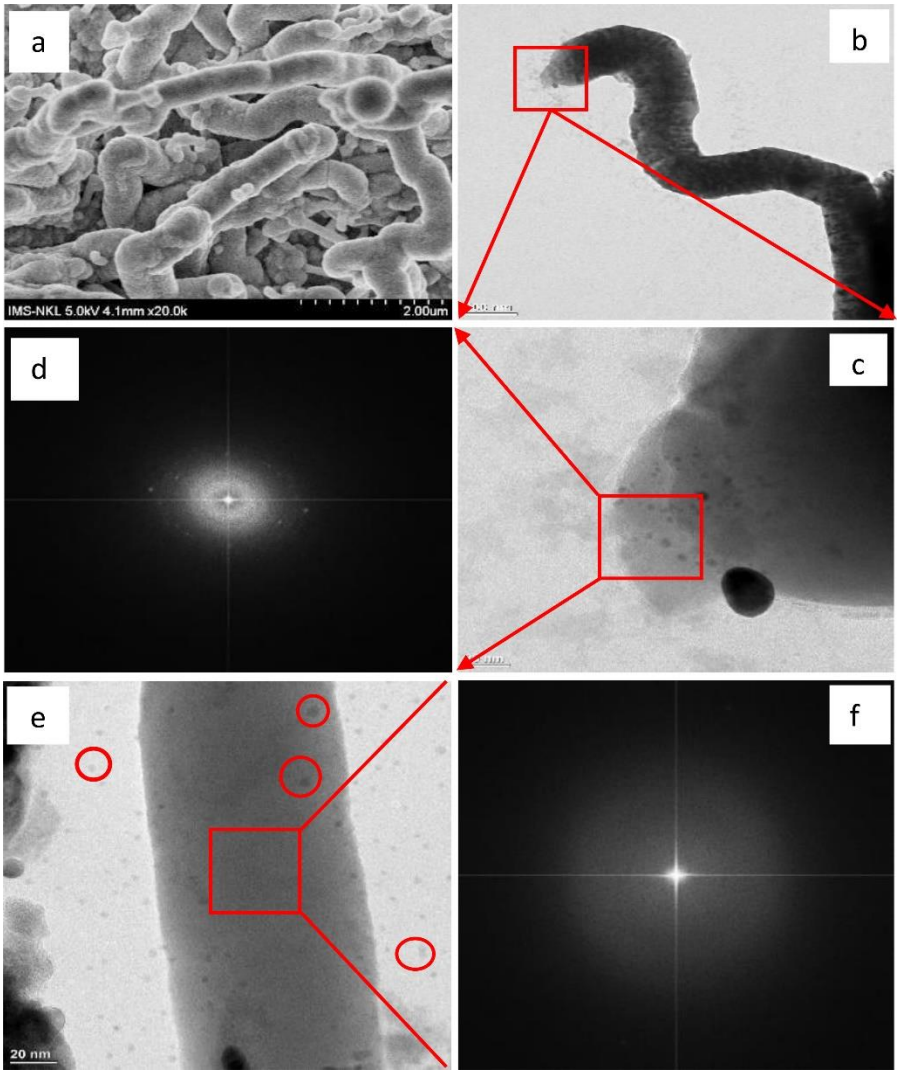

Figure 11 SEM and TEM micrographs of the chemical polishing surface M7 sample: SEM image of NWs configurations on M7 sample (a); the magnificated TEM image of a NW (b); the magnified TEM image of the tip of the NW (c); the red color box indicates place where the FFT was obtained, the structure feature of this region is mainly amorphous (d); the magnified TEM image of a NW part, the result shows that the NW structure has two parts: the shell part has average thickness of 50 nm and the core part has thickness of about 100 nm, both the shell and core parts containing the small crystalline phases (marked grey points) (e) and the FFT result of the NW body is shown to be amorphous structure (f).

Figure 12 (a-d) shows the results of Ge_xO_y configurations grown on M8 chemical polishing surface samples covered with 130 nm Au catalyst layer thickness. Here we see that there are only multifacial configurations of Ge_xO_y grown. *There are pentagonal shapes or six-sided cubes grown with a big uniform size of about 2 µm. We suppose these configurations are considered the nanocrystals (NCs) configurations*. However, this hypothesis should be studied more clearly and in detail. Figure 12e) shows the result of the Energy-dispersive X-ray spectroscopy (EDX) measurement of the Ge_xO_y

multi-facial configuration on M8. From the measured data, we see that the weight % compositions of the Ge: O ratio are both equal to the ratio of 37.51/62.40 = 1:1.6659, i.e., the structure-property of the grown multifacial configuration, in this case, is $Ge_1O_{1.66}$ (x = 1, y = 1,6659 < 2). *The ratio of x to y indexes in Ge_xO_y nanomaterials is a ratio number containing the decimal number, and this feature is usually represented for the nanoscale system. This result is reasonable and could be accepted*. This result could explain that the formation or growth of $Ge_1O_{1.6659}$, in this case, occurred in the poor oxygen environment of the 10^{-1} Torr pressure low vacuum closed tube. We also see that in the case of a very thick Au catalyst layer thickness (130 nm), there are no NWs grown; here, we suppose that the chemical-physical reactions, relative compositions of Ge, O, and the role of Au catalyst in the thick Au layer and Au droplets differ from that in the case of thin Au catalyst layer. In these technological conditions, the nano seems formations and the orientations of Nano seeds for NWs growth did not occur. Consequently, NWs could not grow instead that multiracial configurations formed. This fact much be studied in more detail.

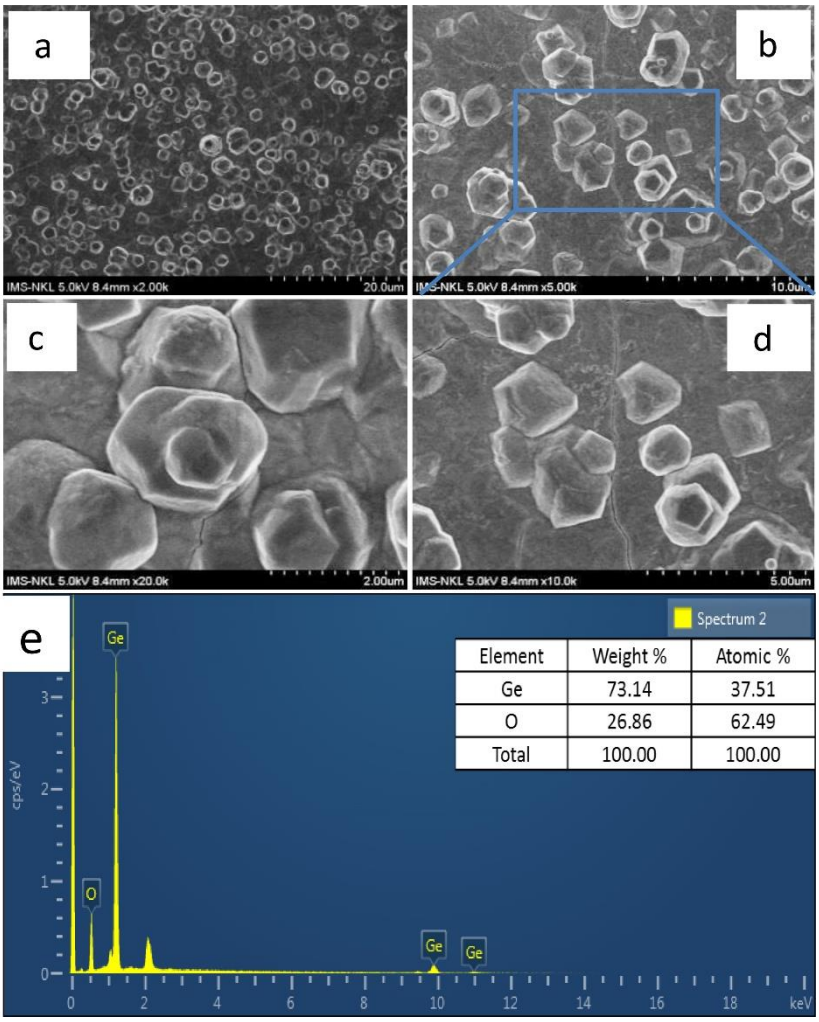

Figure 12 SEM micrographs of Ge_xO_y multifacial configurations grown on Chemical polishing surface M8 sample with 130 nm Au catalysis layer thickness with the different magnifications (a-d) and EDX image of Ge multifacical configuration (e) on M8 sample with the composition $Ge_1O_{1.6659}$ of Ge_xO_y nanomaterials grown on the deep chemical etching surface samples with different Au catalyst layer thickness at different technological conditions.

3.3 The Grown Results of Ge_xO_y Nanomaterials Configurations on the Deep Chemical Etching Surface Samples with Different Au Catalyst Layer Thickness at Different Technological Conditions

Figure 13 shows the nanomaterials grown on the deep chemical etching surface samples containing many defects and larger pits-bumps with no fine surface. Figures 13 (a, b) shows the NWs grown results of the deep chemical etching surface M9 sample in Group 3 with 50 nm Au catalyst layer thickness. Here we see that the sizes of NWs are significant and relatively uniform, with big sphere configurations formed on their tops. The NWs sizes are about 200 nm to 500 nm in diameter with several micrometers (µm) in length. The sizes of big spheres on the NWs tops are about 1 µm to 1.2 µm (Figures 13 a, b, c). *We observed visually that the colors of spheres have the same colors as that of NWs, consequently, we think that the chemical compositions of spheres are the same as that of NWs. The model of the VLS growth method with Oxide Assist Growth mechanism can explain the growth mechanism of NWs in this case* [26, 27].

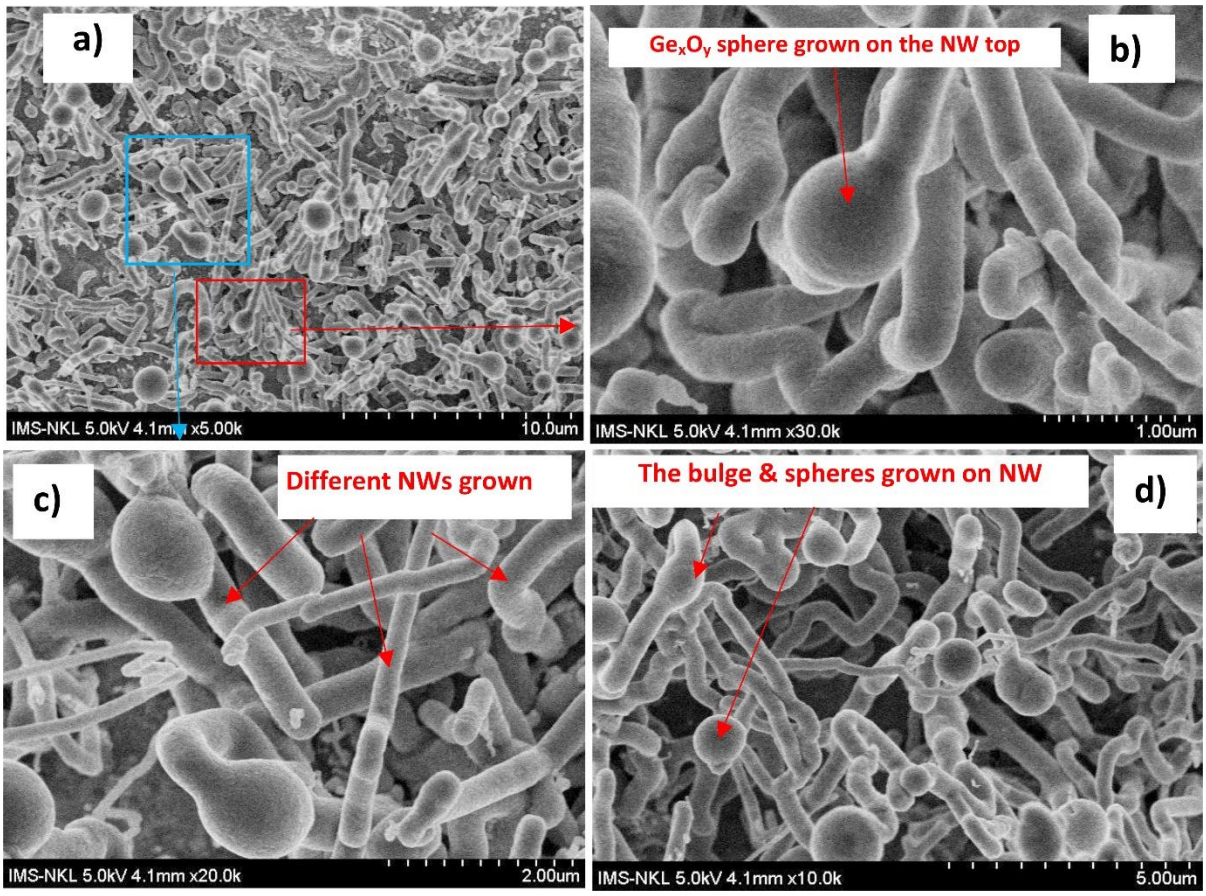

Figure 13 The different magnitificated FESEM micrographs of Ge_xO_y NWs grown on the deep chemical etching surface M9 sample covered with 50 nm Au catalyst layer thickness. SEM micrograph of NWs with two marked boxes in two small regions (a) which are magnified as shown in (b, c). There are big bulges and spheres formed on the tops of NWs (a, b, c, d).

Figure 14 shows TEM micrographs of the grown NWs and structural properties of NW on the tip region in the case of the chemical deep etching surface M9 sample with 50 nm Au catalysis layer thickness. Here the TEM and FFT results show that the NW on the tip region has the structural feature of two parts: the shell or cover layer of NW has a size of about 4-6 nm with an amorphous

phase (Figure 14f) and core parts with crystalline phase Figure 14e).

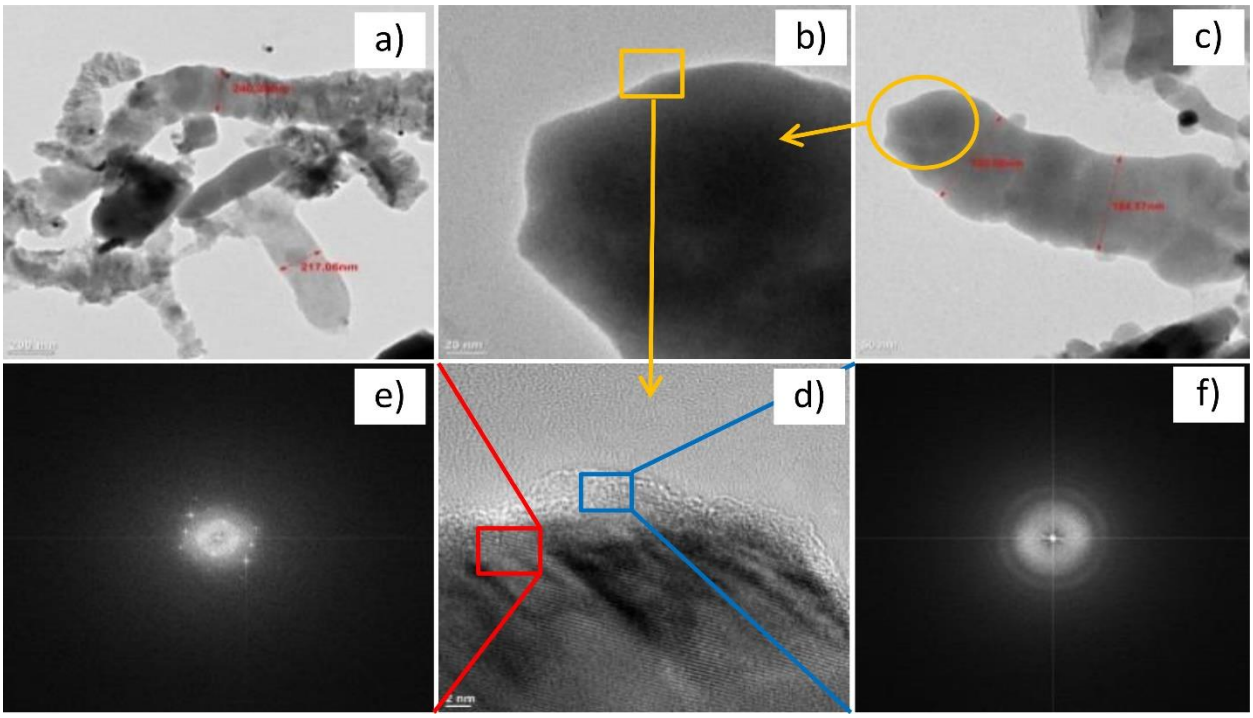

Figure 14 TEM micrographs on the deep etching surface M9 sample with 50 nm Au catalysis layer thickness: a group of nanowires with sizes of 217-240 nm (a); the magnified image of NW top (b); the magnified specific NW image with the diameter size variation from 184.57 nm and 185.66 nm (c); Cross sectional magnified TEM image from the marked small region on the NW's top of (b) this structure consists of the shell and core parts (d). The FFT results on TEM image in shell region showed the structural feature to be amorphous (f), while the TEM image in the core region of NW showing crystalline feature(e).

Figure 15 shows Ge_xO_y nanomaterials configurations grown on the deep chemical etching surface M10 sample with 130 nm Au catalyst layer thickness. There were no NWs, only the multifacial configurations or big spheres, as shown. The sizes of these configurations are in the range of 1 to 1.6 µm. So the thick thickness of Au catalyst layer and surface defects play an essential role in the multifacical configuration of the nanocrystals.

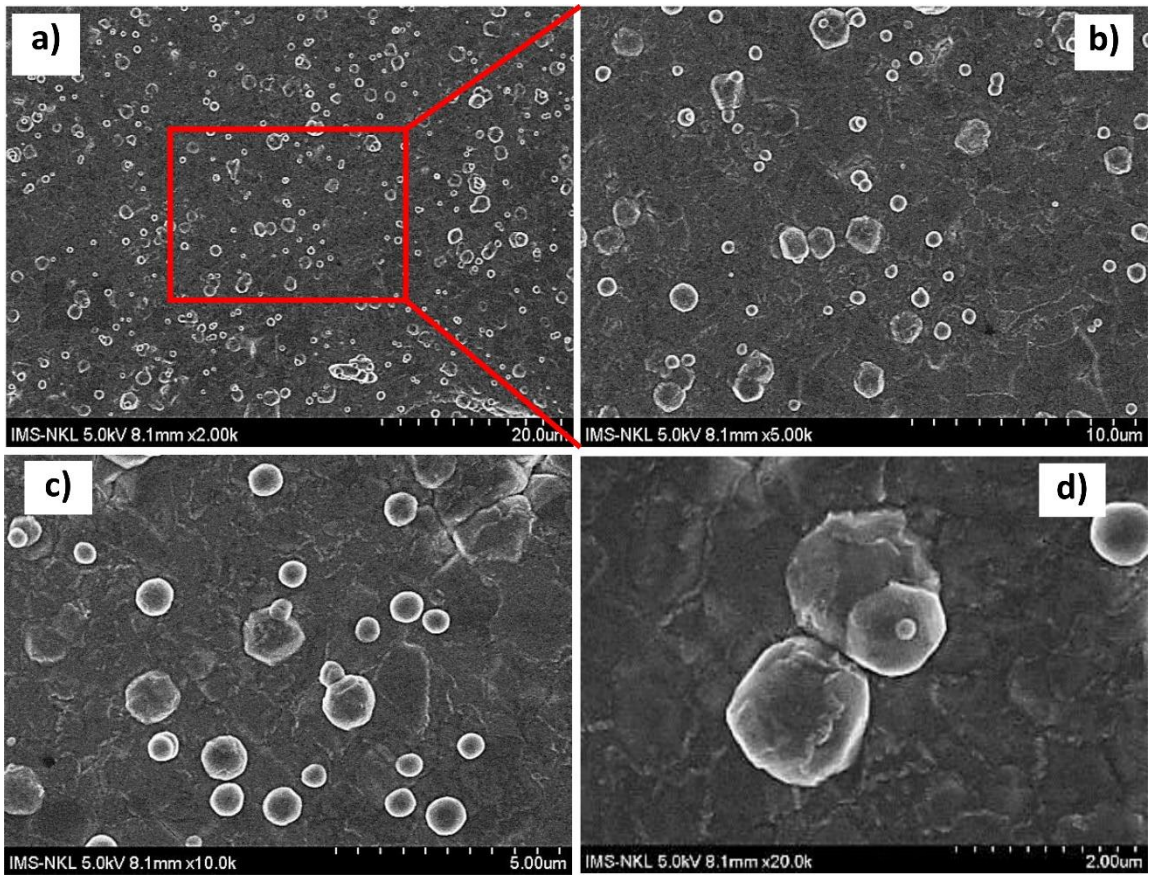

Figure 15 FESEM micrographs of special multifacial configurations grown with different magnifications on M10 sample with 130 nm Au catalysis layer thickness. The sizes of multifacial configurations are about 1.0 µm to 1.6 µm.

Figure 16 shows the TEM micrographs of a multifacial configuration and structural property of its edge part. Here we would like to note that preparing the thin sample for TEM investigation is challenging from the thick sample. Based on the TEM investigated results, we see that there are also two parts: the cover (shell) part with about 5 nm and the core part (Figure 16b). The EDP (Electronic Data Processing) image shows that the structural property of the core part is crystalline (Figure 16c) for the deep chemical etching surface M10 sample with 130 nm Au catalyst thickness.

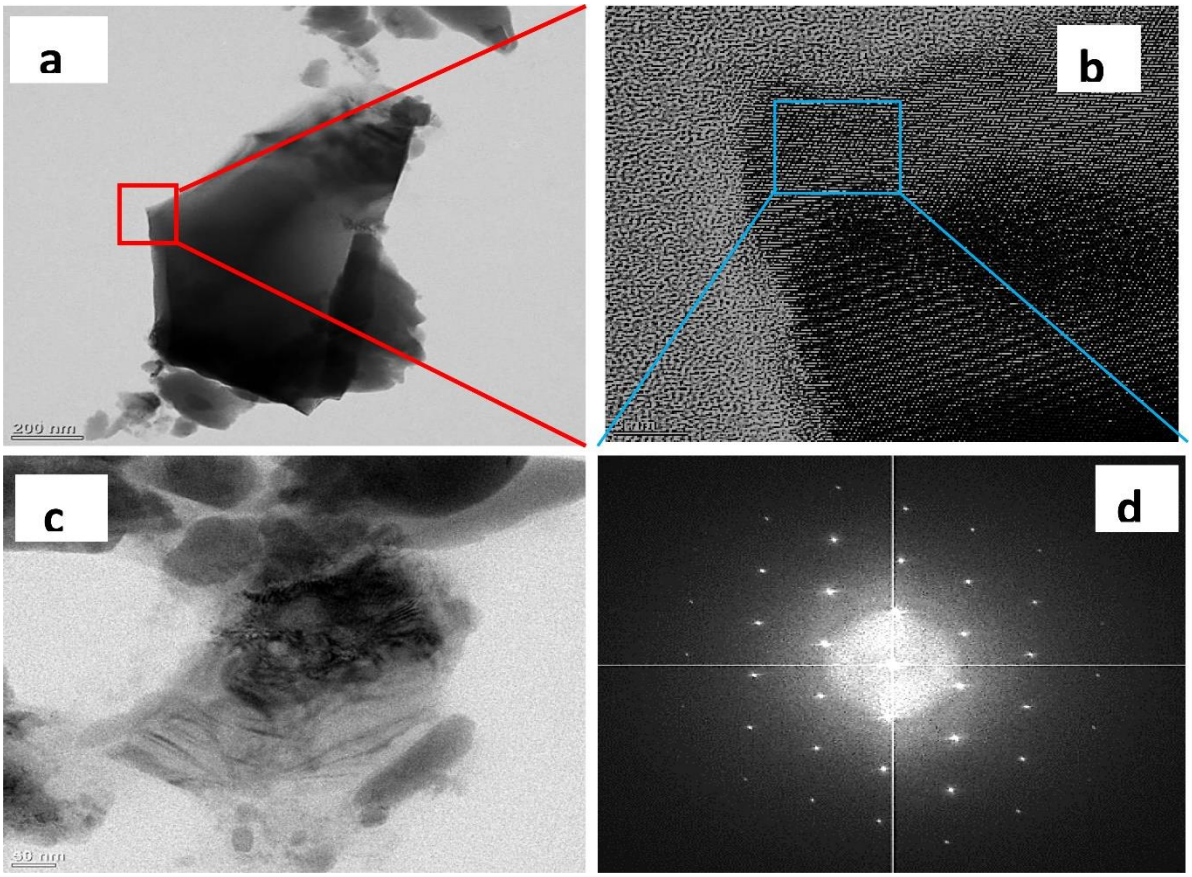

Figure 16 TEM micrographs of the parts from the deep chemical etching surface M10 sample with 130 nm Au catalyst layer thickness: the different magnified images of nano multifacial configuration parts (a, c), the TEM magnified image in the marked box region, this region also consists of two parts of the amorphous phase shell layer and crystalline phase core part (b). The EDP image showed a crystalline structure inside the nano configuration (d).

3.4 The Results of Ge_xO_y Nanomaterials Configurations Grown on the Initial Rough Surface Samples with Different Au Catalyst Layer Thickness at Different Technological Conditions

Regarding the Ge_xO_y nanomaterials growing on the initially rough surface samples containing long traces, grave defect after the slice sawing process and chemically treated by the prepared manufacture company (as seen in Figure 2d) we see that in the case of M11 covered with the 50 nm Au catalyst layer thickness, where the Ge_xO_y NWs have grown with high density. The NWs is about 200 nm in diameter and several μm in length as in Figure 17.

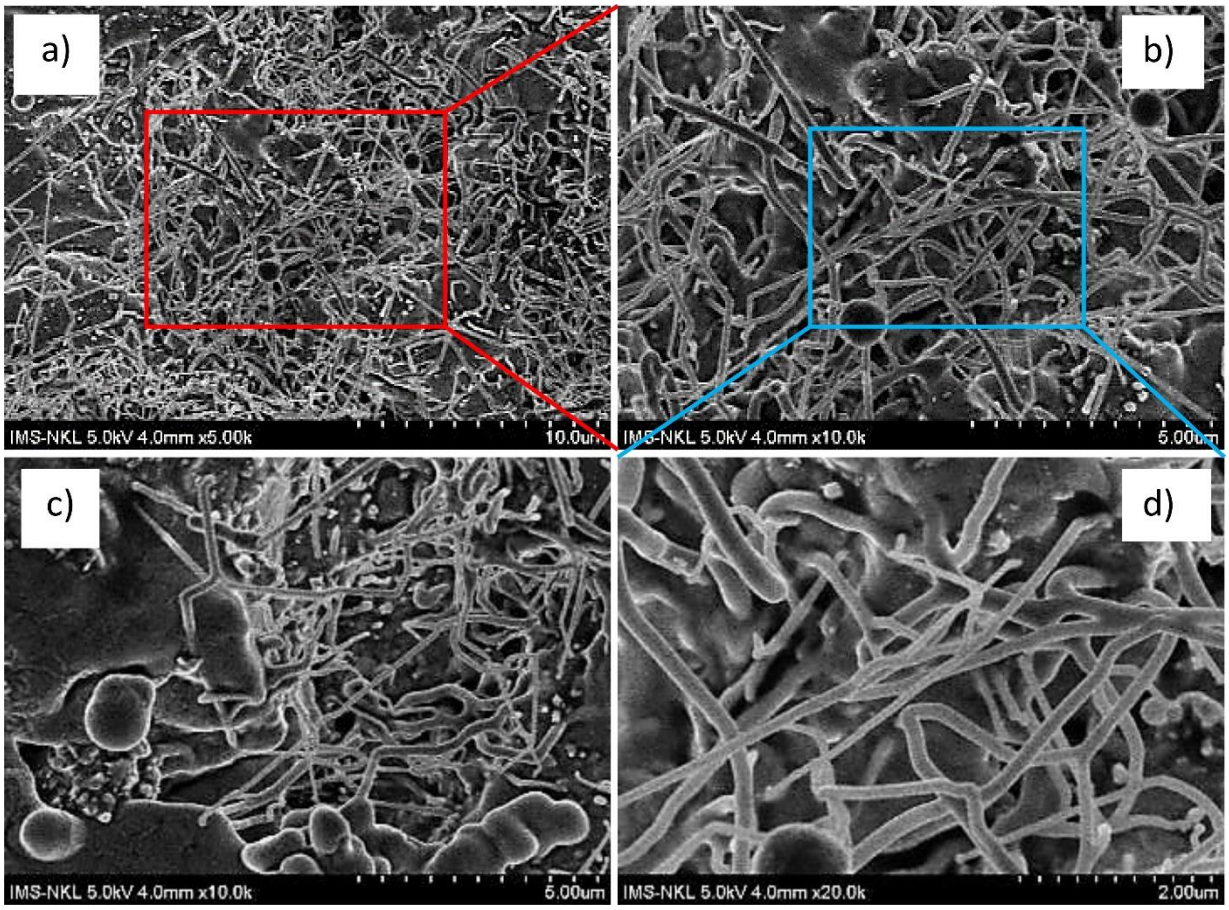

Figure 17 FESEM micrographs of Ge_xO_y NWs configurations grown on sample M11 in the case of the initial rough Surface sample with 50 nm Au catalyst layer at different magnifications.

Figure 18 shows the different magnification FESEM micrographs of the Ge_xO_y multifacial and spheres configurations grown on the initially rough surface M12 sample with the 130 nm Au catalyst layer thickness. Here we see that there are many multifacial configurations grown. There are assumed to be nanocrystal configurations. The structural properties of these configurations have not been investigated, but we think that the structural properties could be the same as the results in previous cases, this means that there are two parts: the shell cover layer with an amorphous phase and the core part with a crystalline phase.

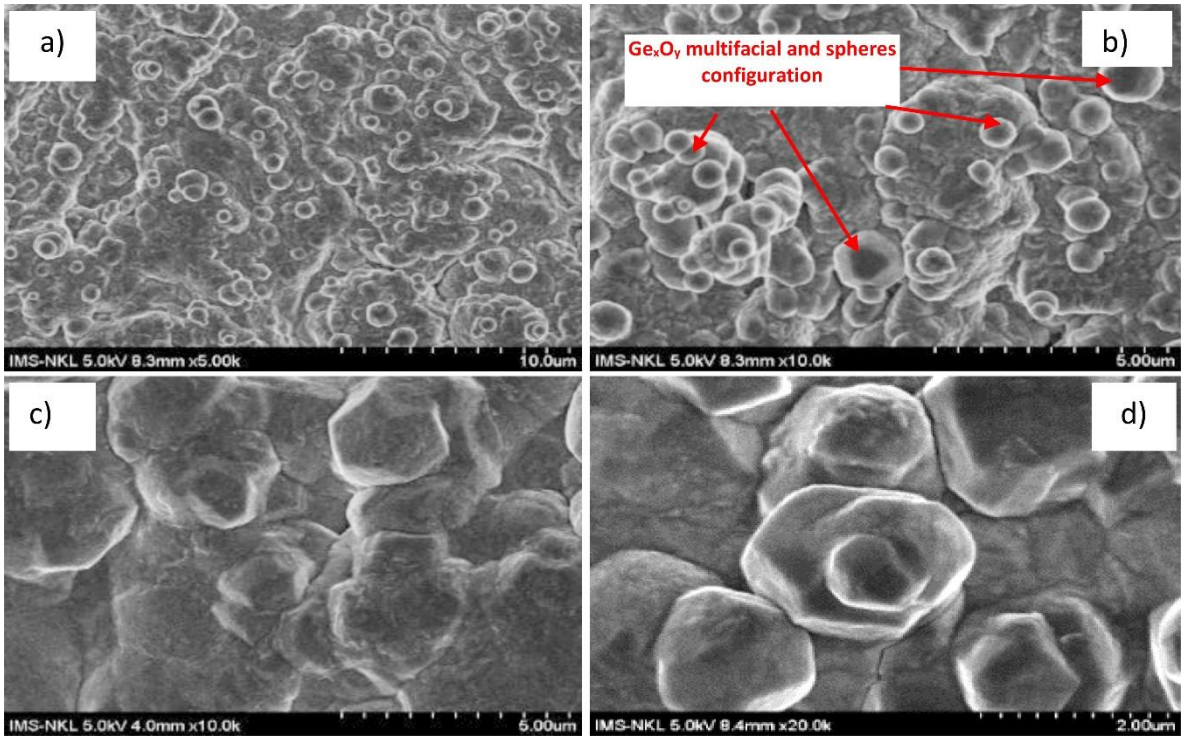

Figure 18 FESEM micrographs of the Ge_xO_y multifacial and spheres configurations with the different magnifications that grown on the initial rough surface M12 sample with the 130 nm Au catalyst layer thickness.

4. Discussion

4.1 On the Effects of Au Catalyst Thickness and Ge Substrate Surfaces States on the Growth of Different Sizes Ge_xO_y Configurations

Firstly, we see the results in comparison briefly: From the obtained results of the Ge_xO_y configurations grown, we see that the grown nanomaterials configurations strongly depend on the Ge substrate surface states and Au catalyst layer thickness.

In the case of thin Au catalyst layer thickness, here we observed that the grown nanomaterials configurations for four different cases of Ge substrate surfaces have common trends of results as the following: In the case of very thin Au catalyst layer thickness (25 nm, 30 nm) covered on the Ge substrate there was only NWs grown with the tangle forms (Figure 4). When Au catalyst layer thickness increased to 50 nm, the growth of the big NWs or the big mixed nanomaterials (NWs, NRs, NPs, and multifacial configurations so-called the NCs) are dominated (Figures 5, 10, 13, 17).

In the case of the thick Au catalyst layer thickness of 130 nm, the pure big multifacial or sphere configurations (Figures 8, 12, 15, 18) were mainly grown. Unfortunately, there are considerable differences in growing processes in four different surface sample groups: Depending on the different Ge substrate surface states with less or more defective surface states, the sizes and morphologies of the grown nanomaterials are different. This means that the defective surface states will strongly determine the NWs, NRs, NPs and NCs configurations' sizes, forms and morphologies. The technological conditions can also control the grown nanomaterials' sizes, forms and morphologies; this means that by the changes in the temperature profiles below or above the

eutectic temperature of Au and Ge binary system, and changes in the Au catalyst layer thickness as well as the thermal annealing times, we can grow different kinds of nanomaterials.

Regarding the effects of the different surface states of Ge substrates (mechanical polishing, chemical polishing, deep chemical etching, and initial rough surfaces as shown in Figure 2), there are a few works studied in Literature [13]. From our obtained results outlined above, we see that the Ge substrate surface states strongly affect the grown Ge_xO_y nanomaterials. For the uniformly fine surface, as in the case of the mechanical polishing surface, the sizes of Au droplets could be formed almost equally; consequently, the almost identical diameters NWs were grown, but for the more defective surface such as the deep chemical etching surface the situation is quite different. This phenomenon could explain as the followings: during the thermal annealing processes, the Au atoms or Au clusters were formed unequally on all Ge substrate surfaces due to the defects caused, some Au atoms and Au tiny droplets have a substantial probability to agglomerate and locate more into the pits-valleys and defective places to form large Au droplets in comparison with that on other places, the Ge and O atoms will diffuse differently into Au droplets being on the defective places and into Au droplets being on free defects surface to form the different sizes Au/Ge/O Nano droplets/clusters on Ge surface, consequently, the different Ge_xO_y nanomaterials grown on the non-defective places and the defective free places. In some cases, there were special configurations of Ge_xO_y (like bulges, spheres or multifacial configurations) that grew from the larger Au/Ge/O nano droplets/clusters situated on the defective places as outlined above section. Here we would like to emphasize that the growths of NWs and multifacial configurations depend on the NW seeds formation and their orientations which still depend on the situations of the supersaturation levels formed on Au/Ge/O droplets/clusters that have reached full or not. Here we can say that the formation and orientation of nano seeds depend on the Au catalyst layer thickness and defective surface states that will determine the formation and grow the different nanomaterials configurations in the later stages.

4.2 The Difference Growth Mechanism between the Formation of NWs and Multifacial, Spheres Configurations

4.2.1 For the Case of NWs Growth

As known, the interface between Au catalysts metal droplets and Ge (111) substrate, this system is achieved by dewetting an Au layer above the Au–Ge eutectic temperature. During thermal annealing on T1 and T2, a large amount of Ge and O atoms will be moved and diffused into the Au droplets to form the different Au-O-Ge droplets with the assistance of the eutectic phase depending on the technological conditions, consequently the Ge_xO_y nanomaterials (NWs, NRs, NPs and NCs) could grow differently.

In the case of thin Au catalyst layer thickness for NWs growth: during the thermal annealing with two steps temperature mode, the nanowires seeds and their orientations were formed and then the growing process will be developed. Their sizes and morphologies will depend on technological conditions. Here the growth mechanism could be explained as follows: during the thermal annealing at T1 and growing T2 temperature above the Eutectic Temperature (361°C) of the Au-Ge system in this case, firstly, the Au catalyst layer disturbed into Au droplets and then diffusion of Ge and O atoms will form Au/Ge/O clusters. Depending on the technological conditions the Au/Ge/O droplets/clusters could reach the supersaturating level or not. In the case of thin Au catalyst layer

thickness, the formed Au droplets are also not so large, the diffusion of Ge atoms and O atoms into Au droplets and Au/Ge/O configurations rapidly reached the supersaturating levels, the nucleation of the NWs seeds will be formed inside the surface Au/Ge/O clusters. The nano configurations (NPs, NWs and NRs) will be grown.

If the Ge substrate surface is a fine, less defective surface and uniform surface, the Au droplets will form uniformly on the whole Ge substrate surface. Consequently, the NWs will grow on the whole Ge surface substrate with uniform sizes.

In the case of a defective Ge substrate surface, the Au droplets will form and agglomerate more in the defective places with larger sizes; the Ge atoms and O atoms diffuse into larger Au droplets to form larger Au/Ge/O configurations but the supersaturating levels could reach slowly or not depending on technological conditions. Consequently, the larger NWs including several special bulges or spheres could be grown and formed from the larger Au/Ge/O configurations in the defective places.

Concerning the growth mechanism of Ge_xO_y NWs, many works have been explaining different growth mechanisms for Ge nanowires growth at the different conditions below, above or just at the eutectic temperature of Ge-Au compositions such as the initial VLS mechanism [3-5], vapor-solid-solid (VSS) mechanism, self-catalytic growth (SCG) mechanism where the SCG mechanism uses without a FECA, and oxide-assisted growth (OAG) mechanism where the VLS mechanism makes use of a foreign element catalytic agent (FECA) [11, 21, 26, 27]. Depending on the growth mechanism, whether the metal element (Au) or the concerning elements taking part in the growth process will be presented in the forms of sphere-semispherical or oxide tips that are often located on the top of the nanowire [25-27]. The growing mechanism for the growth of big NWs together with several unique configurations such as bulges and spheres located on the NWs tops could be explained by the OAG mechanism.

So far although there were a series of investigations done, there were also many vital features of the OAG (Oxide Assisted Growth) mechanism that still need to be fully understood, and a unified model for the growth mechanism of NWs still needs to be investigated [26-32].

4.2.2 For the Case of Multifacial, Spheres Configurations Growth

Concerning the growth of the multifacial spheres configurations so-called nanocrystals (NCs) and their features we would like to mention several points concerned: A nanocrystal is a material particle having at least one dimension smaller than 100 nm, based on quantum dots (or a nanoparticle), and composed of atoms in either a single or poly-crystalline arrangement meanwhile the concept of a nanocrystalline (NC) material is commonly defined as a crystallite (grain) size below 100 nm. Grain sizes from 100–500 nm are typically considered "ultrafine" grains. By other definition forms: A nanocrystal is a material particle having at least one dimension smaller than 100 nm, based on quantum dots (a nanoparticle) and composed of atoms in either a single- or poly-crystalline arrangement. The applications of semiconductor nanocrystals promise to play a significant role in several new technologies, which gives rise to their potential use in the fields of nonlinear optics, luminescence, electronics, catalysis, solar energy conversion, and optoelectronics, as well as other areas [29, 30]. So far many works are studying the different aspects of Ge nanocrystalline, nanocrystals concerning the synthesis methods [31-40]. Based on these definitions with their properties and the basis of the grown experiment results of the multifacial and spheres

configurations as shown in Figures 8, 12, 15, and 18, in addition to the obtained results of TEM investigations being on Figures 8, 16 we could say that the grown multifacical and spheres configurations, in this case, are the nanocrystals configurations.

The growth mechanism concerning the formation of NCs configurations here we suppose that when Au catalyst layer thickness is increased to a thickness of 130 nm, the large Au droplets and then the Au/Ge/O configurations will be formed after annealing processes on T1 and T2 temperatures. Due to the larger Au droplets, the diffusion of Ge and O atoms into Au/Ge/O configurations is difficult to reach rapidly to the supper saturation levels, consequently, instead of NWs seeds, the NCs seeds are formed in the different Au/Ge/O configurations, then the instead NWs, NRs growth, the NCs configurations grown as shown in Figures 8, 12, 15, and 18 in the above sections. Indeed, the formation of NCs in this case must be studied more clearly and in detail.

The results of big NWs grown together with the formations of the Ge_xO_y big bulges, spheres located on the tops of NWs as shown in Figures 5, 10, and 13 could not be explained by the initial simple VLS mechanism [6], the growing mechanism in this case could be considered a typical case of the foreign Au catalyst element mediated Oxide Assisted Growth – OAG with the vapor-solid-solid (vapor-solid) mechanism that is vapor-quasisolid-solid (vapor-quasi liquid-solid) mechanism proposed by the works of S. Noor Mohammad et.al. [26, 27].

The variation of the structural properties of Ge_xO_y for NWs or NCs where x and y values could get the unit number or decimal number, this results could be explained due to there is the plenty or lack of Oxygen atoms being in the growth environment leading to the plenty or lack of Oxygen atoms being in the Au/Ge/O droplets/clusters growing NWs or NCs. These processes lead to the different phase transitions in Au-Ge liquid at the above Eutectic Temperature of Au-Ge alloy during the growth process, resulting in different structural properties and morphologies.

Indeed, the formation and growth of very big NPs and NCs configurations from the different surface states is a challenging problem to explain. This should be studied in more detail.

5. Conclusions

This paper outlined the development of technological processes using the thermal VLS method with two steps temperature mode over the Eutectic Temperature of Au and Ge binary system to grow the different Ge nanomaterials on the different Ge substrate surface states after that some investigations of structural morphologies, chemical compositions have also outlined.

When the Ge substrate surface is fine in the mechanical polishing surface sample and the Au catalyst layer thickness is smaller than 30 nm, the grown nanomaterials are mainly NWs with tangle forms, the growth mechanism is pure initial VLS mechanism.

The different Ge substrate surface states strongly affected the formation of different sizes and morphologies of Ge_xO_y nanomaterials, including NWs, NPs, NRs, and NCs. We grew the different sizes and configurations of NWs or mixed nanomaterials of NWs, NPs, and NRs as well as the multifacial configurations like nanocrystals by choosing the suitable Au layer thickness of about 50 nm, and 130 nm and technological conditions. The influences of the Ge substrate surface states were investigated. The more pits etching or defects, the more significant the nanomaterials configurations grown are in comparison with the fine surface-mechanical polishing surface.

In the case of the thickness of the Au catalyst layer is increased to 50 nm, the bigger NWs were grown mainly in all cases of different Ge substrate surfaces, but in the case of the more defective

surface states, the mixed Ge_xO_y nanomaterials including NWs, NRs, NPs, and NCs were grown simultaneously, this result is explained by the effect of surface states where Au atoms were agglomerated to form bigger Au droplets leading to growing bigger NWs together with bulges spheres formation located on the NWs tops. The growth mechanism, in this case, can be explained by the vapor-solid-solid (vapor-solid) mechanism that is a typical case of the foreign Au catalyst element mediated Oxide Assisted Growth (OAG).

In the case of the Au catalyst layer thickness increased to a high value of 130 nm, the big multifacial and/or spheres configurations, so-called the NCs formed in almost case. The obtained TEM results showed that the grown NCs configurations contain two parts: the core part has a crystalline phase, and the sheath-skin part has a size of 3 nm to 10 nm with an amorphous oxide phase. The formation of NCs could explain by the NCs seeds having formed instead of NWs seeds.

The NWs and NCs configurations of Ge_xO_y have a ratio composition of decimal numbers, the growth mechanism of NCs, and the formation of the bulges and spheres located on the NWs tops are hard to explain clearly. These problems should be continued to research more clearly next time.

Acknowledgments

This work is carried out partly in the Institute of Materials Sciences (IMS) –VAST and partly in the Institute of Theoretical and Application Research (ITAR), Duy Tan University. The Authors express their thanks to the Leaders of the Institutions who have given some facilities to conduct experiments.

The authors also would like to thanks Ph. D student Nguyen Tien Thanh (IMS) for several experiments arrangements in research period at IMS-VAST.

Author Contributions

Author's inputs into the manuscript are described as the following:

Prof. Khac An DAO: Leader project, outline conceptions of manuscript and manuscript composition, writing manuscript.

MSc. Pham Hong Trang: doing experiments, analyzing experiment data, reading and checking revising the errors in manuscript.

Ph.D. Hoang Van Vuong: carrying out TEM measurements.

Funding

This research was funded partly by the National Foundation of Science and Technology Development (NAFOSTED for the basic research project (103.02.-2017.346) in 2018- 2021 period to carry out some parts of these researches.

Competing Interests

The authors declare that we have no competing interests in connection to the manuscript and certify that we have NO affiliations with or involvement with any financial interest in the subject matter in this manuscript.

References

1. Pitkethly MJ. Nanomaterials-the driving force. Mater Today. 2004; 7: 20-29.
2. Kim J. Nanodevices by using semiconductor nanowires. University of Texas at Austin; 2004.
3. Charitidis CA, Georgiou P, Koklioti MA, Trompeta AF, Markakis V. Manufacturing nanomaterials: From research to industry. Manuf Rev. 2014; 1: 11.
4. Beser AS. Nanotechnology fabrication methods. Nanotechnology. 2016; ET 1039.
5. Heath JR, LeGoues FK. A liquid solution synthesis of single crystal germanium quantum wires. Chem Phys Lett. 1993; 208: 263-268.
6. Schwalbach EJ, Voorhees PW. Phase equilibrium and nucleation in VLS-grown nanowires. Nano Lett. 2008; 8: 3739-3745.
7. Lu H, Meng X. Nanophase diagram of binary eutectic Au-Ge nanoalloys for vapor-liquid-solid semiconductor nanowires growth. Sci Rep. 2015; 5: 11263.
8. Li C, Mizuta H, Oda S. Growth and characterization of Ge Nanowires by chemical vapor deposition. In: Nanowires - Implementations and Applications. InTech; 2011. pp 487-507. doi: 10.5772/18991.
9. Užupis A, Tyczkowski J, Gubiec K, Tamulevičius S, Andrulevičius M, Pucėta M. Properties of Ge_xO_y: H thin films produced by plasma-assisted chemical vapor deposition. Mater Sci. 2009; 15.
10. Zhang YF, Tang YH, Wang N, Yu DP, Lee CS, Bello I, et al. Silicon nanowires prepared by laser ablation at high temperature. Appl Phys Lett. 1998; 72: 1835-1837.
11. Zhu Z, Song Y, Zhang Z, Sun H, Han Y, Li Y, et al. The vapor-solid-solid growth of Ge nanowires on Ge (110) by molecular beam epitaxy. arXiv. doi: 10.48550/arXiv.1706.01605.
12. Wu Y, Yang P. Germanium nanowire growth via simple vapor transport. Chem Mater. 2000; 12: 605-607.
13. Panciera F, Chou YC, Reuter MC, Zakharov D, Stach EA, Hofmann S, et al. Synthesis of nanostructures in nanowires using sequential catalyst reaction. Nat Mater. 2015; 14: 820-825.
14. Nguyen P, Ng HT, Meyyappan M. Growth of individual vertical germanium nanowires. Adv Mater. 2005; 17: 549-553.
15. Marshall AF, Goldthorpe IA, Adhikari H, Koto M, Wang YC, Fu L, et al. Hexagonal close-packed structure of Au nanocatalysts solidified after Ge nanowire vapor-liquid-solid growth. Nano Lett. 2010; 10: 3302-3306.
16. Minaye Hashemi FS, Thombare S, Morral AF, Brongersma ML, McIntyre PC. Effects of surface oxide formation on germanium nanowire band-edge photoluminescence. Appl Phys Lett. 2013; 102: 251122.
17. Micoulaut M, Cormier L, Henderson GS. The structure of amorphous, crystalline and liquid GeO_2. J Phys. 2006; 18: R753.
18. Wolter SD, Tyler T, Jokerst NM. Surface characterization of oxide growth on porous germanium films oxidized in air. Thin Solid Films. 2012; 522: 217-222.
19. Huang S. Open-framework germanates and nickel germanates: Synthesis and characterization. Sweden: Department of Materials and Environmental Chemistry Stockholm University; 2012.
20. Hajjar S, Garreau G, Josien L, Bubendorff JL, Berling D, Mehdaoui A, et al. Morphology and composition of Au catalysts on Ge (111) obtained by thermal dewetting. Phys Rev B. 2011; 84: 125325.

21. Gamalski AD, Tersoff J, Kodambaka S, Zakharov DN, Ross FM, Stach EA. The role of surface passivation in controlling Ge nanowire faceting. Nano Lett. 2015; 15: 8211-8216.
22. Lee SF, Lee LY, Chang YP. Controlled growth of germanium nanowires via a Solid–Liquid–Solid (SLS) mechanism. Adv Mat Res. 2012; 557: 523-529.
23. Kodambaka S, Tersoff J, Reuter MC, Ross FM. Germanium nanowire growth below the eutectic temperature. Science. 2007; 316: 729-732.
24. Liang J, Xu K, Fan LJ, Huang Y. The synthesized principle and property of several extraction agents for germanium. Adv Mat Res. 2012; 455: 624-629.
25. Wang D. Synthesis and properties of germanium nanowires. Pure Appl Chem. 2007; 79: 55-65.
26. Noor Mohammad S. For nanowire growth, vapor-solid-solid (vapor-solid) mechanism is actually vapor-quasisolid-solid mechanism. J Chem Phys. 2009; 131: 224702.
27. Noor Mohammad S. Investigation of the oxide-assisted growth mechanism for nanowire growth and a model for this mechanism. J Vac Sci Technol B. 2008; 26: 1993-2007.
28. Dao KA, Pham HT, Nguyen TT, Phan AT. The formation mechanism and model of the surface nanoscale Kirkendall effect on Au catalyst island/GaAs substrate by thermal Vapor-Liquid-Solid method with two-step temperature mode. Catalysts. 2019; 9: 1072.
29. Suryanarayana C. Structure and properties of nanocrystalline materials. Bull Mater Sci. 1994; 17: 307-346.
30. Trindade T, O'Brien P, Pickett NL. Nanocrystalline semiconductors: Synthesis, properties, and perspectives. Chem Mater. 2001; 13: 3843-3858.
31. Zhang B, Xiang Y, Shrestha S, Green M, Conibeer G. Growth mechanism and surface structure of Ge nanocrystals prepared by thermal annealing of cosputtered GeSiO ternary precursor. J Nanomater. 2014; 2014: 31.
32. Capan I, Carvalho A, Coutinho J. Silicon and germanium nanocrystals: Properties and characterization. Beilstein J Nanotechnol. 2014; 5: 1787-1794.
33. Bonafos C, Carrada M, Benassayag G, Schamm-Chardon S, Groenen J, Paillard V, et al. Si and Ge nanocrystals for future memory devices. Mater Sci Semicond Process. 2012; 15: 615-626.
34. Sasani Ghamsari M, Tarkhorani S. Colloidal synthesis of germanium nanocrystals. Nano Res. 2017; 2: 172-178.
35. Inoue A, Hashimoto K. Amorphous and nanocrystalline materials: Preparation, properties, and applications. Berlin: Springer; 2001.
36. Haubold T. Nanocrystalline materials – structure and properties. Magn Prop Fine Particles. 1992; 67-75. doi: 10.1016/B978-0-444-89552-3.50014-1.
37. Carolan D. Recent advances in germanium nanocrystals: Synthesis, optical properties and applications. Prog Mater Sci. 2017; 90: 128-158.
38. Zhao J, Yang L, McLeod JA, Liu L. Reduced GeO_2 nanoparticles: Electronic structure of a nominal GeO_x complex and its stability under H_2 annealing. Sci Rep. 2015; 5: 17779.
39. Muflikhun MA, Castillon GB, Santos GNC, Chua AY. Micro and nano silver-graphene composite manufacturing via horizontal vapor phase growth (HVPG) technique. Mater Sci Forum. 2017; 901: 3-7.
40. Muflikhun MA, Chua AY, Santos GN. Statistical design analysis of silver-titanium dioxide nanocomposite materials synthesized via horizontal vapor phase growth (HVPG). Key Eng Mater. 2017; 735: 210-214.